

Direct measurement of the London penetration depth in $\text{YBa}_2\text{Cu}_3\text{O}_{6.92}$ using low-energy μSR

R. F. Kiefl,^{1,2,3} M. D. Hossain,^{1,2} B. M. Wojek,^{4,5} S. R. Dunsiger,⁶ G. D. Morris,² T. Prokscha,⁴ Z. Salman,⁴ J. Baglo,¹ D. A. Bonn,^{1,3} R. Liang,^{1,3} W. N. Hardy,^{1,3} A. Suter,⁴ and E. Morenzoni⁴

¹*Department of Physics and Astronomy, University of British Columbia, Vancouver, British Columbia, Canada V6T 1Z1*

²*TRIUMF, 4004 Wesbrook Mall, Vancouver, British Columbia, Canada V6T 2A3*

³*Canadian Institute for Advanced Research, Toronto, Canada*

⁴*Paul Scherrer Institut, Labor für Myon-Spin Spektroskopie, CH-5232 Villigen PSI, Switzerland*

⁵*Physik-Institut der Universität Zürich, CH-8057 Zürich, Switzerland*

⁶*Physik Department E21, Technische Universität München, D-85748 Garching, Germany*

(Received 4 March 2010; published 7 May 2010)

A direct measurement of the London penetration depth in the high- T_c superconductor $\text{YBa}_2\text{Cu}_3\text{O}_{6.92}$ has been made using low-energy μSR with an effective background suppression method. The average magnetic field versus mean depth was measured in the Meissner state of high-purity detwinned crystals of $\text{YBa}_2\text{Cu}_3\text{O}_{6.92}$. The resulting magnetic field profiles along the a and b axes are consistent with a local London model beyond 10 nm but there are deviations close to the surface. The absolute values of λ_a and λ_b extrapolated to zero temperature are $126.1 \pm 1.2 \pm 3$ and $105.5 \pm 1.0 \pm 3$ nm, respectively. These results are compared with other less direct methods and extend the use of low-energy μSR to small crystals.

DOI: [10.1103/PhysRevB.81.180502](https://doi.org/10.1103/PhysRevB.81.180502)

PACS number(s): 74.25.Uv, 74.25.Ha, 76.60.-k, 76.75.+i

One of the fundamental quantities of a superconductor is the London penetration depth, λ , which is the characteristic length scale that a magnetic field penetrates into the surface of a superconductor while in the Meissner state.¹ In the clean limit the absolute value of λ is directly related to the superfluid density n_s via $1/\lambda^2 = \mu_0 e^2 n_s / m$ and consequently its variation as a function of temperature, doping and orientation are of central importance in testing microscopic theories of exotic superconductors. For example, the linear variation in $1/\lambda^2$ with respect to temperature was a key finding confirming the d -wave nature of the pairing in $\text{YBa}_2\text{Cu}_3\text{O}_{6+x}$.^{2,3} Also, early μSR studies of the vortex phase in polycrystalline samples found a linear correlation between $1/\lambda^2$ and T_c in the underdoped region.⁴⁻⁶ More recent measurements on crystals both in the Meissner⁷ and vortex states⁸ indicate this systematic variation with doping is sublinear and may be connected with an approach to a quantum-critical point.^{7,9} The large in-plane anisotropy of λ in $\text{YBa}_2\text{Cu}_3\text{O}_{6.95}$ measured with IR reflectivity,¹⁰ was taken as evidence for a multiband effect, whereby a one-dimensional Fermi sheet associated with the CuO chains in $\text{YBa}_2\text{Cu}_3\text{O}_{6.95}$ contributes to the superfluid flowing in the chain direction.¹¹ This is a unique feature of $\text{YBa}_2\text{Cu}_3\text{O}_{6+x}$ which distinguishes it from other cuprates. Accurate measurements of the absolute value of λ and its anisotropy are required to clarify central issues in $\text{YBa}_2\text{Cu}_3\text{O}_{6+x}$ and more generally in the area of exotic superconductors.

Unfortunately, accurate measurements of λ are difficult due to many possible systematic uncertainties. For example, in any bulk measurement the assumption of an exponential decay of the field in the Meissner state is only valid in the local London limit of a perfect surface.¹ This adds uncertainty to all bulk measurements where the field profile is assumed and not measured. Alternatively, one can determine λ from μSR studies in the vortex state where the muon acts as a sensitive probe of the magnetic field distribution.^{8,12,13} However, in this case the nonlocal and nonlinear effects complicate the theory¹⁴ leading to an effective-field-dependent penetration depth. Until now there has been no

way to verify to what extent this effective penetration depth reflects the true λ in the Meissner state. The most direct method is to measure the field profile and λ in the Meissner state using a beam of low energy muons. This requires no *a priori* knowledge of the superconducting state. However, until now this has only been possible on large area polycrystalline films^{15,16} where the doping and scattering are not well defined. In this Rapid Communication we report a direct measurement of the magnetic field profile in an oriented mosaic of the latest generation of high-purity crystals of $\text{YBa}_2\text{Cu}_3\text{O}_{6.92}$ using low-energy μSR . An effective background suppression method was developed to extend low-energy μSR to studies of small crystals. We observe an exponential decay of the magnetic field and corresponding supercurrent density deep inside the crystals. The results for the absolute value of λ and its anisotropy are compared with previous less direct methods for measuring λ .

The freshly grown crystals of $\text{YBa}_2\text{Cu}_3\text{O}_{6.92}$ were made by the self-flux method using BaZrO_3 crucibles.¹⁷ The purity of this latest generation of crystals is the same as for crystals in which quantum oscillations in resistivity have recently been reported.¹⁸ Superconducting quantum interference device measurements indicate that the average superconducting T_c was 94.1 K with a spread of less than 0.1 K. Each of the crystals was approximately rectangular in shape with lateral dimensions in the ab plane ranging from 1 to 3 mm and a thickness in the c direction ranging from 0.1 to 0.3 mm. They were detwinned to a level greater than 95%. The total area of the mosaic was 55 mm². The crystal faces were mirrorlike in appearance and atomic force microscopy indicates the roughness of the surface to be a few nm.

The experiment was performed at the Paul Scherrer Institute on the μE4 beamline,¹⁹ where the low-energy muons are produced at a rate of about $10^4/\text{s}$ using a solid Ar moderator capped with 12 nm of N_2 . After emerging from the moderator with an average energy of about 20 eV, the low-energy muons are accelerated to 15 keV, and transported electrostatically to the μSR spectrometer located 2.2 m away. The entire transport system as well as the spectrometer are main-

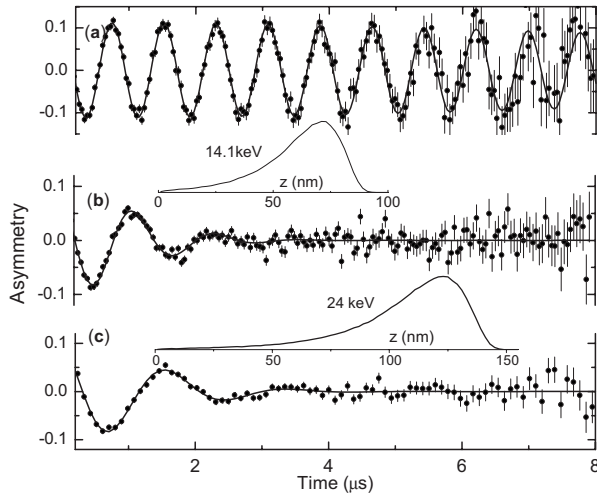


FIG. 1. (a) The muon spin precession signal in the normal state of $\text{YBa}_2\text{Cu}_3\text{O}_{6.92}$ at 110 K in an external field of 9.46 mT applied parallel to the a direction. The mean implantation energy is $E = 14.1$ keV which corresponds to a mean implantation depth of 62.8 nm. (b) The same conditions as (a) except in the superconducting state at $T = 8$ K. The inset shows the calculated stopping distribution. (c) The same conditions as (b) except the energy of implantation is increased to 24 keV.

tained in an UHV environment. Incoming muons are detected with a thin carbon foil trigger detector and reach the entrance to the cryostat with a mean energy of 14.1 keV and an asymmetric energy spread of 0.42 keV. The implantation energy is varied by applying a voltage to the sample holder, which is electrically isolated from the cryostat via a sapphire plate. Further details on the low-energy muon production, the beam transport and the spectrometer can be found elsewhere.²⁰ Implantation profiles are calculated with TRIM.SP ion implantation code taking into account the spread in energy and incident angle of muons reaching the sample.²¹ The reliability of this code to calculate muon implantation profiles has been tested in separate measurements.²² The uncertainty in the mean implantation depth in $\text{YBa}_2\text{Cu}_3\text{O}_{6.92}$ is estimated to be about 2% of the mean depth (~ 2 nm) and is the largest source of systematic uncertainty in the absolute values for λ_a and λ_b reported here. The crystals were attached to a high-purity Al sample holder coated with 1 μm of Ni. Since the Ni is ferromagnetic, muons which miss the sample experience a large hyperfine field²³ and thus are removed from the frequency window of interest. Consequently, there is no detectable background precession signal close to the free Larmor frequency. This very effective background suppression method was the critical step which allows low-energy μSR to be applied to crystals much smaller than the beam diameter. The external magnetic field was applied parallel to the surface in the ab plane and perpendicular to the beam direction.

Examples of the muon precession signals in the crystal mosaic may be seen in Fig. 1. Figure 1(a) shows the muon precession signal in the normal state at 110 K in a small magnetic field of 9.46 mT applied along the a axis of the crystals with an implantation energy at 14.1 keV. The amplitude of the precession is less than the maximum instrumental

asymmetry of 0.28 due to the fact that about 40% of the muons land in the mosaic while the remaining 60% end up in the polycrystalline Ni film coating on the sample holder. Control experiments on a Ag disk the same size as the sample showed that the magnetic perturbation from such a thin layer of Ni has no effect on the precession signal in the sample under study. This is evident from Fig. 1(a) where the observed frequency corresponds to the applied field with a damping rate of $(0.086 \pm 0.011) \mu\text{s}^{-1}$ which is consistent with the expected damping from host Cu nuclear dipole moments. All measurements in the superconducting state were carried out under zero-field-cooled conditions in order to avoid flux trapping at the surface. Meissner screening of the external field is apparent by comparing the normal state [Fig. 1(a)] with the superconducting state [Fig. 1(b)]. Note that, in addition to the increased damping rate, there is also a clear reduction in the average precession frequency or internal field in the superconducting state. The depth dependence of the average internal field is evident by comparing Figs. 1(b) and 1(c) which have different implantation profiles (see insets). The curves in Figs. 1(b) and 1(c) are generated from fits to a London model profile:

$$B(z) = \begin{cases} B_0 \exp[-(z-d)/\lambda_{a,b}] & z \geq d \\ B_0 & z < d, \end{cases} \quad (1)$$

where B_0 is the magnitude of the applied field, $\lambda_{a,b}$ is the magnetic penetration depth in the a or b direction, respectively, z is the depth into the crystal, and d is an effective dead layer inside of which the supercurrent density is suppressed. A theoretical muon precession signal $\mathcal{A}(t)$ at each energy was generated by taking the signal from a particular depth z and then averaging over the calculated stopping distribution $\rho(z)$

$$\mathcal{A}(t) = A \exp[-\sigma^2 t^2 / 2] \int \rho(z) \cos[\gamma_\mu B(z)t + \phi] dz, \quad (2)$$

where γ_μ is the muon gyromagnetic ratio, A is the initial amplitude of precession, ϕ is the initial phase of the incoming muon spins, and σ is a parameter which takes into account any inhomogeneous broadening. Well below T_c , σ is about $0.6 \mu\text{s}^{-1}$ and is dominated by bulk magnetization effects, whereby flux expelled from neighboring crystals broadens the magnetic field distribution at the surface of any given crystal. This is confirmed by the fact that σ remains temperature independent up until around $0.8T_c$ and then decreases rapidly as one approaches T_c , as expected from bulk magnetization effects. The parameter σ also has a weak energy dependence and is only weakly correlated with λ_a and λ_b .

Figure 2 shows the average local field [$\langle B \rangle = \int \rho(z) B(z) dz$] determined from fits at a single energy as a function of beam energy (bottom scale) and corresponding mean implantation depth (top scale). The filled circles and open diamonds are from data taken with the shielding currents flowing along the a and b axes, respectively, (or equivalently the magnetic field along the b and a axes, respectively). The corresponding curves are generated from a global fit of runs taken at 8 K for both orientations and all

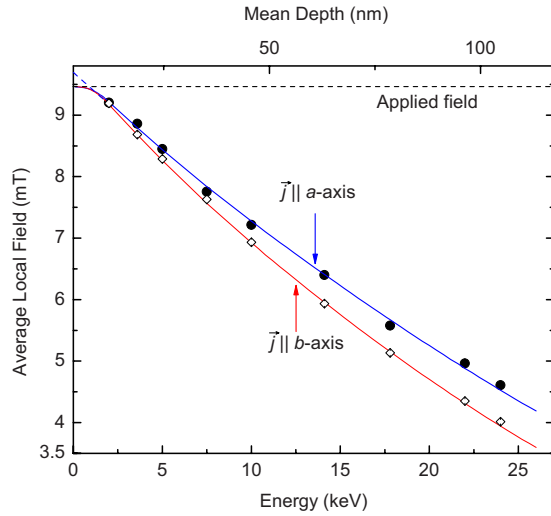


FIG. 2. (Color online) The average magnetic field versus mean stopping depth in an applied field of 9.46 mT such that the shielding currents are flowing in the a direction ($\vec{j} \parallel a$, filled circles) and b direction ($\vec{j} \parallel b$, open diamonds). The curves are the average fields generated from a global fit of all the spectra at 8 K taken at all energies and for both orientations.

energies using the calculated TRIM.SP implantation profiles.²¹ A few examples of implantation profiles are shown as insets in Fig. 1. The common parameters are $\lambda_a = 128.9(1.2)$ nm, $\lambda_b = 108.4(1.0)$ nm, and $d = 10.3(5)$ nm. Statistical uncertainties are determined from the global χ^2 surface and take into account the strong correlation between $\lambda_{a,b}$ and d . Since there is almost no correlation between d and λ_a/λ_b , this ratio is determined more accurately than the absolute values of λ_a and λ_b as shown in the first row of Table I. Our model provides an excellent fit to the data as indicated by the fact that the χ^2 per degree of freedom is 1.05. This is also evident from Fig. 2 which shows the average field falls exponentially from the surface for higher implantation energies. Some deviation from a simple exponential is evident from the curvature in the fitted curve at the lowest energies, required so that the field at the surface equals the applied field. This implies that the supercurrent density is suppressed near the surface relative to a London model. We have modeled this in the simplest possible way by assuming a dead layer d with no

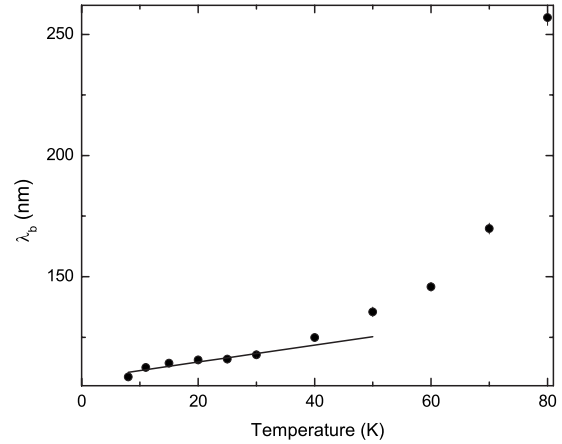


FIG. 3. Temperature dependence of the London penetration depth in an external magnetic field of 9.46 mT applied parallel to the a axis so that the shielding currents are in the b direction and parallel to the CuO chains.

supercurrent. This is idealized but the nature of the data does not warrant more complicated models. It is unclear to what extent this suppression of the supercurrent density is intrinsic as a result of the discontinuous nature of electronic properties near a surface. There are no other measurements of electromagnetic properties as a function of depth in $\text{YBa}_2\text{Cu}_3\text{O}_{6.92}$ crystals to compare with. Surface sensitive techniques such as scanning tunnel microscopy and angle resolved photoemission spectroscopy (ARPES) are only sensitive to the top few unit cells where the properties can be very different than in the bulk. Finally, we note a suppression of the supercurrent density was reported in a previous low-energy μSR study of the field profile in a thin film of $\text{YBa}_2\text{Cu}_3\text{O}_{6.92}$ and attributed to surface roughness.¹⁵ It is difficult to exclude such extrinsic effects which could also lead to a suppression of the supercurrent density near a surface. Measurements on atomically flat cleaved surfaces are needed to resolve the true origin of d .

The absolute value of λ_b as a function of temperature is shown in Fig. 3. The data points are the fitted values of λ_b determined from a fit to the model in Eq. (2) at a single implantation energy of 22 keV. Since d is not temperature dependent it was fixed at the value determined by the global

TABLE I. Measurements of the absolute value of the magnetic penetration depth ($\lambda_{a,b}$) in $\text{YBa}_2\text{Cu}_3\text{O}_{6.92}$. Average magnetic penetration depth $\lambda_{ab} = \sqrt{\lambda_a \lambda_b}$. The vortex lattice measurements are quoted without systematic errors.

λ_a (nm)	λ_b (nm)	λ_{ab} (nm)	λ_a/λ_b	Comment
$126 \pm 1.2 \pm 3$	$105.5 \pm 1.0 \pm 3$	$115.3 \pm 0.8 \pm 3$	1.19 ± 0.01	This work
		118 ± 0.4		Conventional μSR in vortex state ^a
		146 ± 3		Low-energy μSR in thin film at 20 K ^b
160	100	126.5	1.6	IR reflectivity at 10 K ^c
103 ± 8	80 ± 5	91 ± 7	1.29 ± 0.07	ESR on Ortho-I $\text{YBa}_2\text{Cu}_3\text{O}_{6.995}$ ^d
		150 ± 10	1.16 ± 0.02	μSR at 10 K ^e
		138 ± 5	1.18 ± 0.02	SANS at 10 K ^f

^aReference 8.

^bReference 15.

^cReference 10.

^dReference 7.

^eReference 24.

^fReference 25.

fit at 8 K. Although the temperature dependence we measure is less precise than obtained from cavity perturbation techniques the method may be used to provide an important confirmation in regard to its accuracy. Systematic errors are most problematic in measurements of the absolute value of λ but they can also affect the measured temperature variation. The solid line is a linear fit of our data below 30 K and gives a slope of 0.35(7) nm/K. This was used to extrapolate our measurement of λ_b at 8 K down to zero temperature. The slope and extrapolated value depend slightly on the fitted temperature range adding an additional systematic error of about 1 nm. The same procedure was used to extrapolate λ_a to 0 K.

The first row in Table I gives our results for λ_a and λ_b in $\text{YBa}_2\text{Cu}_3\text{O}_{6.92}$ extrapolated to $T=0$. The first error is the statistical uncertainty at 8 K whereas the second is a systematic uncertainty associated with the extrapolation to 0 K and the muon stopping distribution. At the moment, the latter dominates the overall uncertainty but should improve with refinements of the stopping distribution calculations. For comparison, we have also included measurements of $\lambda_{a,b}$ in $\text{YBa}_2\text{Cu}_3\text{O}_{6.92}$ from other less direct methods. There is surprisingly good agreement with the bulk μSR measurement of the average in plane penetration depth in the vortex state on a previous generation of crystals. In that case λ_{ab} was obtained by extrapolating the measurement of an effective field dependent λ in the vortex state down to zero magnetic field.⁸ Until now there has been no way to test the accuracy of this extrapolation into the Meissner state. The agreement is remarkable considering there are several phenomenological parameters required to fit the data in the vortex state. The value obtained in this work is considerably shorter than that for a $\text{YBa}_2\text{Cu}_3\text{O}_{6.92}$ film.¹⁵ However, the difference is understandable since the reduced T_c of the film (87.5 K) indicates the doping level is much different than in the crystals. Also we find that the anisotropy is considerably less than found in early IR reflectivity measurements which first revealed the large anisotropy in λ . It is also less than reported for Gd-doped Ortho-I phase ($x=6.995$, $T_c=89$ K) but we anticipate that the anisotropy and λ are a strong function of doping.¹⁰ The anisotropy from the current work is close to vortex state measurements using μSR (Ref. 24) and small-angle neutron scattering (SANS) on a large detwinned crystal

of optimally doped $\text{YBa}_2\text{Cu}_3\text{O}_{6.92}$.²⁵ This may be fortuitous since the effective ab penetration depth in this early generation of crystal appears to be considerably longer than in the current generation of high purity crystals. The current method should make it possible to study in much greater detail how the intrinsic λ and its anisotropy evolve as a function of doping in $\text{YBa}_2\text{Cu}_3\text{O}_{6+x}$ and other exotic superconductors.

In summary we have used low-energy μSR with an effective background suppression method to make a direct measurement of the magnetic field profile in the Meissner state of a mosaic of small detwinned single crystals of $\text{YBa}_2\text{Cu}_3\text{O}_{6.92}$. The measured λ_a and λ_b are in surprisingly good agreement with average value of the in-plane magnetic penetration depth λ_{ab} obtained from conventional μSR studies of the vortex state of an earlier generation of crystals. This suggests that the effective-field-dependent penetration depth in the vortex state, at least in this one case, extrapolates to the actual London penetration depth in the Meissner state to within an accuracy of a few percent. The in-plane anisotropy $\lambda_a/\lambda_b=1.19\pm 0.01$ is considerably less than reported from early IR studies and is similar to that found in electron spin resonance (ESR) studies on Gd-doped $\text{YBa}_2\text{Cu}_3\text{O}_{6.995}$ although the current measurement is far more accurate than either previous value. The measured anisotropy agrees with early μSR and SANS experiments on a much earlier generation of crystal but this is likely fortuitous since the absolute values for λ_a and λ_b in that study are much longer than reported in the current study. The field profiles are exponential on the scale of λ but there are deviations close to the surface which are not yet understood. Most importantly we have demonstrated that low-energy μSR can be used to study fundamental properties of small crystals. This will greatly increase the scientific impact of low-energy μSR in the study of exotic superconductors.

We would like to acknowledge helpful discussions with Jeff Sonier. This research was supported by the Paul Scherrer Institute, the Natural Sciences and Engineering Research Council of Canada and the Canadian Institute for Advanced Research. We would especially like to acknowledge H. P. Weber for his expert technical support.

¹C. P. Poole *et al.*, *Superconductivity*, 2nd ed. (Academic Press, New York, 1995).

²W. N. Hardy *et al.*, *Phys. Rev. Lett.* **70**, 3999 (1993).

³J. E. Sonier *et al.*, *Phys. Rev. Lett.* **72**, 744 (1994).

⁴Y. J. Uemura *et al.*, *Phys. Rev. Lett.* **62**, 2317 (1989).

⁵Y. J. Uemura *et al.*, *Phys. Rev. Lett.* **66**, 2665 (1991).

⁶A. J. Drew *et al.*, *Phys. Rev. Lett.* **101**, 097010 (2008) and references therein.

⁷T. Pereg-Barnea *et al.*, *Phys. Rev. B* **69**, 184513 (2004).

⁸J. E. Sonier *et al.*, *Phys. Rev. B* **76**, 134518 (2007).

⁹D. M. Broun *et al.*, *Phys. Rev. Lett.* **99**, 237003 (2007).

¹⁰D. N. Basov *et al.*, *Phys. Rev. Lett.* **74**, 598 (1995).

¹¹W. A. Atkinson, *Phys. Rev. B* **59**, 3377 (1999).

¹²J. E. Sonier *et al.*, *Rev. Mod. Phys.* **72**, 769 (2000).

¹³A. Maisuradze *et al.*, *J. Phys.: Condens. Matter* **21**, 075701 (2009).

¹⁴M. H. S. Amin *et al.*, *Phys. Rev. B* **58**, 5848 (1998).

¹⁵T. J. Jackson *et al.*, *Phys. Rev. Lett.* **84**, 4958 (2000).

¹⁶A. Suter *et al.*, *Phys. Rev. Lett.* **92**, 087001 (2004).

¹⁷R. Liang *et al.*, *Physica C* **304**, 105 (1998).

¹⁸N. Doiron-Leyraud *et al.*, *Nature (London)* **447**, 565 (2007).

¹⁹T. Prokscha *et al.*, *Nucl. Instrum. Methods Phys. Res. A* **595**, 317 (2008).

²⁰E. Morenzoni *et al.*, *Physica B* **289-290**, 653 (2000).

²¹W. Eckstein, *Computer Simulation of Ion-Solid Interactions* (Springer, Berlin, 1991).

²²E. Morenzoni *et al.*, *Nucl. Instrum. Methods Phys. Res. B* **192**, 254 (2002).

²³K. Nagamine *et al.*, *Hyperfine Interact.* **1**, 517 (1975).

²⁴C. Ager *et al.*, *Phys. Rev. B* **62**, 3528 (2000).

²⁵S. T. Johnson *et al.*, *Phys. Rev. Lett.* **82**, 2792 (1999).